Human response to the noise emissions of an isolated propeller under turbulent inflow conditions

Merino Martinez, R.; Quaroni, L.N.

Publication date
2025

Document Version
Final published version

Published in
Proceedings of the 54th International Congress and Exposition on Noise Control Engineering

Human response to the noise emissions of an isolated propeller under turbulent inflow conditions

Roberto Merino-Martinez[1] and Luca Nicola Quaroni[2]
Faculty of Aerospace Engineering, Delft University of Technology
Kluyverweg 1, 2629 HS Delft, The Netherlands

ABSTRACT

Psychoacoustic listening experiments were conducted to investigate the human response to propeller noise under turbulent inflow conditions. The sound stimuli considered were recorded in aeroacoustic wind tunnel experiments featuring an isolated six-bladed propeller. The propeller operated under different isotropic inflow turbulence conditions and collective blade pitch angles. Higher inflow turbulence intensity levels caused a growth in the broadband noise emissions of the propeller, increasing the overall loudness levels. On the other hand, sharpness and tonality consistently decreased due to the increase in low-frequency noise and the tone-masking effect by the aforementioned broadband noise, respectively. The listening experiments aimed to elucidate the effect of these contradicting trends on sound perception. It was observed that lower noise annoyance ratings were reported for higher inflow turbulence intensity levels and lower collective blade pitch angles. Overall, only the tonality metric provided a statistically significant correlation with the annoyance ratings, indicating the importance of this perceptual aspect in propeller noise, in combination with loudness and sharpness. Other energy-based sound metrics, like the effective perceived noise level, failed to correctly describe the results of the listening experiment. In general, this analysis is valuable for the perception-influenced design of devices equipped with propellers.

1. INTRODUCTION

A growing number of modern systems incorporate propellers, including drones [1], urban air mobility (UAM) vehicles [2,3], and advanced aerospace technologies such as distributed electric propulsion [4] and boundary layer ingestion systems [5]. As a result, there has been growing research interest in recent years in understanding propeller noise emissions [6,7] and, from a psychoacoustic perspective, how these are perceived by humans [8,9]. This has led to the development of perception-driven design strategies aimed at minimizing noise annoyance during operation [10].

To simplify experimental setups, most aeroacoustic studies focus on isolated propellers operating in a controlled environment, typically in anechoic chambers [10, 11] or wind tunnels [7], and assume clean, low-turbulence inflow conditions. However, in real-world applications, propellers are often installed close to the airframe, where they are exposed to turbulent inflow generated by

[1]r.merinomartinez@tudelft.nl (corresponding author)

[2]l.n.quaroni@tudelft.nl

upstream structures [12]. While a number of studies have investigated this scenario [6, 13], the current understanding of the effects of inflow turbulence on propeller noise, particularly broadband noise and its perceptual implications, remains limited.

Recent research [14] performed a psychoacoustic characterization using perception-based sound quality metrics (SQMs) on an isolated propeller tested in aeroacoustic wind tunnel measurements featuring varying levels of isotropic inflow turbulence and different collective blade pitch angles β. Overall, higher values of loudness for increasing levels of inflow turbulence were reported, whereas other SQMs, such as tonality or sharpness, experienced a decrease. These variations are partly explained, respectively, by the increase in broadband noise due to the turbulence ingestion and corresponding leading edge noise. This, in turn, masks to some extent the presence of the tonal components (i.e. make them be perceived as less prominent) and causes higher levels of low-frequency noise in the propeller noise signature. Nevertheless, the combined effect of these contradicting trends in the perceived annoyance remains unclear. The current study addresses this gap by conducting psychoacoustic listening experiments to elucidate how these phenomena affect the perceptual human response to the same sound stimuli.

Section 2 briefly documents the experimental setup employed in the aeroacoustic wind tunnel measurements, as well as the acoustic equipment and test conditions used. The conventional and psychoacoustic sound metrics employed in this study are listed in section 3. Details about the listening experiment campaign, including the facility, the test subjects, and sound stimuli, are provided in section 4. The main results are discussed in section 5, and the conclusions are drawn in section 6.

2. AEROACOUSTIC WIND-TUNNEL EXPERIMENTS

The anechoic, open-jet wind tunnel (A-Tunnel) at Delft University of Technology [15] was employed for conducting the aeroacoustic measurements of the propeller under evaluation. The circular outlet of the wind tunnel (exit diameter of 600 mm) located on the floor of the facility has a contraction ratio (CR) of 15. An additional axisymmetric nozzle with an exit diameter D_{ext} of 420 mm was attached on top of the outlet, see Fig. 1, increasing the overall CR to approximately 30.

The propeller employed was made of steel and had six blades with a diameter D_p equal to 203.2 mm (8"). The blades can be manually adjusted in terms of collective pitch angle β. In the current study, β values (measured at 70% of the blade span) of 25°, 27.5°, 30°, and 32.5° were investigated [6]. This propeller (normally referred to as X-PROP-S) has been the subject of several publications; for its geometry, including spinner and nacelle dimensions, the reader is referred to [16]. For the current experiments, the propeller was placed at a distance of 252 mm ($0.6\,D_{ext}$) from the exit plane of the nozzle. For more detailed information about this experimental setup, the interested reader is referred to [6].

Since the default configuration of the A-tunnel presents very low turbulence intensities [15], three different turbulence grids were employed to generate additional turbulence and evaluate different inflow conditions. The grids consisted of planar squared meshes made of aluminum plates with a thickness of 5 mm. The grids were placed at the junction between the axisymmetric nozzle and the wind tunnel outlet on the floor, see Fig. 1. The three grids (named henceforth A, B, and C) had the same open area ratio of 64% but different values for the bar width d and mesh length M, see Table 1 and Fig. 1. These differences in grid geometries provide several combinations of turbulence intensity TI (defined as the ratio between the root-mean-square velocity fluctuations u'_{rms} and the freestream velocity in the streamwise direction U_∞) levels and streamwise turbulence integral length scales Λ. Table 1 presents these values for a freestream velocity U_∞ of 30 m/s and a streamwise distance of $x = 0.4\,D_{ext}$ downstream of the nozzle exit, i.e., upstream of the propeller plane. The values for the baseline grid-off case are also presented in the same table as a reference. All these values were obtained using hot-wire anemometry measurements [6].

The far-field noise emissions of the propeller were measured using a phased array containing 63 free-field microphones (not considered here) and a directivity arc containing 8 microphones, see

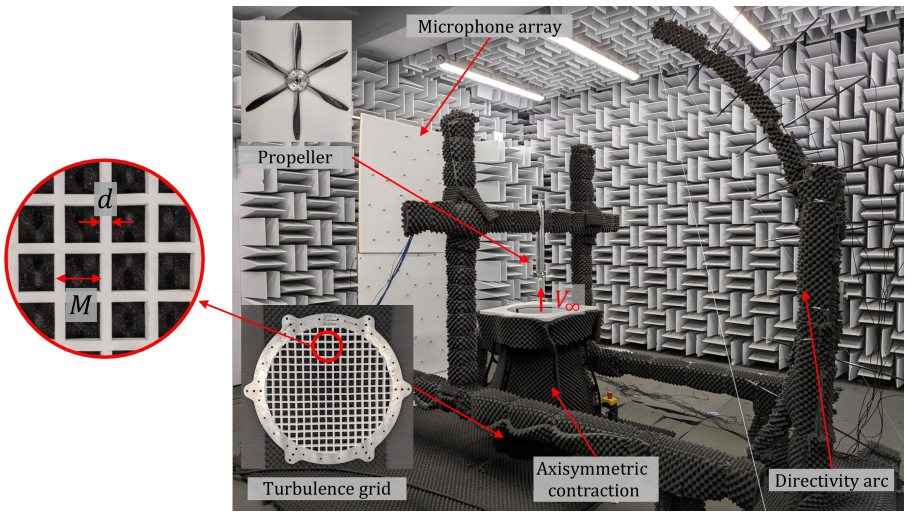

Figure 1: Experimental setup in the A-tunnel for the aeroacoustic measurements [14].

Table 1: Bar width d, mesh length M, turbulence intensity TI, and streamwise turbulence integral length scales Λ for each of the turbulence grids at a distance $x = 0.4\,D_{ext}$ downstream of nozzle exit for U_∞ of 30 m/s [6].

Grid	**d, [mm]**	**M, [mm]**	**TI, [%]**	**Λ, [mm]**
Off	N/A	N/A	< 0.1	N/A
A	7	35	1.97	11.4
B	10	50	2.75	14.1
C	12	60	3.44	16.2

Fig. 1. The directivity arc spanned an emission angle range of 70° from $\theta = 70°$ to 140°, with $\theta = 90°$ corresponding to the rotor disk plane and $\theta = 0°$ to the upstream direction. Both arrays of microphones were positioned at a distance of 1.3 m ($\approx 6.5\,D_p$) from the propeller's axis, with the directivity arc centered at the propeller's rotation center. To account for the sound convection due to the flow, the acoustic data recorded was corrected in terms of amplitude and polar emission angle θ, following the guidelines explained in [17]. A sampling frequency of 51200 Hz and a recording time of 60 s were employed, which corresponds to approximately 10,000 propeller rotations acquired per operating condition.

Acoustic absorbent materials (melamine and pyramidal polyurethane foam panels, see light and dark gray surfaces in Fig. 1) were placed over all exposed surfaces within the anechoic plenum to reduce potential acoustic reflections [18]. The turbulence grids were also equipped with 20-mm-thick melamine foam panels, which were water-jet cut to the respective grid geometry and glued onto the downstream side to suppress both secondary reflections and the generation of tones by vortex-shedding mechanisms [19].

3. CONVENTIONAL AND SOUND QUALITY METRICS

Conventional sound metrics normally employed in noise assessment pose challenges for quantifying noise annoyance [9]. Nonetheless, current noise regulations continue to employ these metrics in order to enforce environmental noise laws. Hence, the current study considers the equivalent sound pressure level $L_{\mathrm{p,eq}}$, its A-weighted version $L_{\mathrm{p,A,eq}}$, as well as the maximum tone-corrected perceived noise level ($\mathrm{PNLT}_{\mathrm{max}}$), and the effective perceived noise level (EPNL) to assess the propeller noise emissions. The

latter two metrics are typically employed during aircraft noise certification processes [20].

In contrast to the sound pressure level L_p metric, which quantifies the purely physical magnitude of sound based on the pressure fluctuations, SQMs aim to describe the subjective perception of sound by human hearing. Therefore, SQMs are expected to capture the auditory behavior of the human ear in a better way than conventional sound metrics. The five most commonly-used SQMs [21] are:

- Loudness (N): Perception of sound magnitude corresponding to the overall sound intensity.
- Tonality (K): Perceived strength of unmasked tonal energy within a complex sound.
- Sharpness (S): High-frequency sound content.
- Roughness (R): Hearing sensation caused by modulation frequencies between 15 Hz and 300 Hz.
- Fluctuation strength (FS): Assessment of slow fluctuations in loudness with modulation frequencies up to 20 Hz, with maximum sensitivity for modulation frequencies around 4 Hz.

These five SQMs were calculated for each sound stimuli and combined into global psychoacoustic annoyance (PA) metrics following the model proposed by Zwicker [22], More [23], and Di *et al.* [24]. Henceforth, the top 5% percentiles of these metrics (values exceeded 5% of the time) are reported (and hence the sub-index *5*). All the conventional sound metrics, SQMs, and the PA metrics were computed using the open-source MATLAB toolbox SQAT (Sound Quality Analysis Toolbox) v1.2 [25].

4. LISTENING EXPERIMENTS

4.1. Experimental setup

The listening experiment campaign was performed at PALILA, the Psychoacoustic Listening Laboratory at the Faculty of Aerospace Engineering of Delft University of Technology [26]. PALILA consists of a box-in-box soundproof booth with interior dimensions of 2.32 m (length) × 2.32 m (width) × 2.04 m (height). The interior walls, ceiling, and part of the floor are covered with acoustic-absorbing foam panels to prevent sound reflections, see Fig. 2(a). Two bass traps are positioned in diagonally opposing corners to minimise low-frequency noise inside the facility. The facility offers free-field sound propagation conditions for frequencies higher than or equal to 1600 Hz and a reverberation time of only 0.07 s. The facility has a weighted average transmission loss of 45 dB and an A-weighted overall background noise level of 13.4 dBA.

The sound reproduction equipment employed consists of a *Dell Latitude 7340* laptop equipped with a touchscreen and connected to a pair of *Sennheiser HD560s* open-back headphones. This equipment is calibrated up to 10 kHz, using a *G.R.A.S. 45BB-14 KEMAR* head-and-torso simulator with *G.R.A.S. KB5000/KB50001 Anthropometric Pinnae*. The reproduction system employs an open-source, Python-based Graphical User Interface (GUI) [27], allowing the experiment to be self-guided and self-paced.

After a short briefing, participants began the experiment with a questionnaire about their age, gender, employment, and education, as well as questions regarding their self-reported hearing health and state of well-being. Participants then proceeded to listen to the sound stimuli and were asked (after listening to each stimulus): "*When you imagine that this is the sound situation in your garden or outdoors, what number from 0 to 10 best shows how much you would be bothered, disturbed, or annoyed by it?*" using an 11-point ICBEN scale. After every four sound samples, participants were given a mandatory 10-s break from listening to alleviate fatigue to some extent. After completing the experiment, the participants were provided a 10-euro universal voucher to compensate for their time.

4.2. Sound stimuli

Given the relatively high similarity within the sound stimuli and the time limitations in listening experiments (mainly to avoid participant fatigue), a representative down-selection of the data

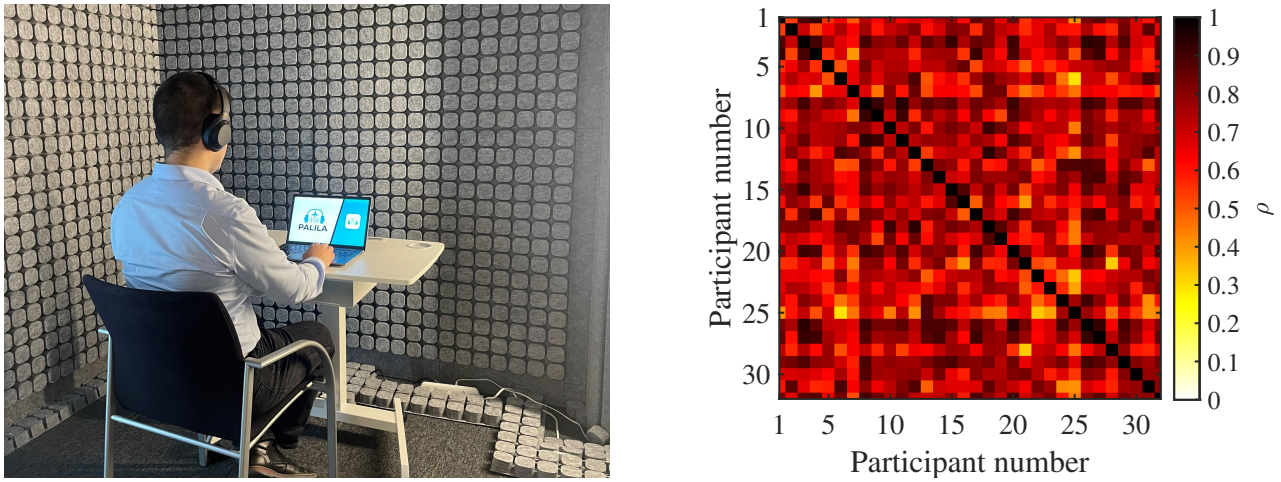

(a) (b)

Figure 2: (a) Example of a listening experiment inside of PALILA. (b) Matrix showing the Pearson correlation coefficients (ρ) between the responses of each pair of individual participants.

measured in the aeroacoustic wind tunnel experiments was performed. The results presented in this paper correspond to a freestream velocity U_∞ of 30 m/s and a rotational frequency f_r of 166.76 Hz, resulting in a tip Mach number $M_{\text{tip}} = V_r/c_0$ of 0.325, where $V_r = \sqrt{(\pi f_r D_p)^2 + U_\infty^2}$ and $c_0 = 340$ m/s is the speed of sound at 16°C. To prevent excessive sound exposure, the experimental acoustic signals recorded in the wind tunnel measurements were scaled down by −20 dB before being used as stimuli in the listening experiment.

In order to investigate the influence of the inflow turbulence intensity TI on the sound perception, stimuli corresponding to the four grid cases (including the Grid off baseline) and a collective blade pitch angle β of 30° were tested. On the other hand, to evaluate the variations with respect to β, all four collective blade pitch angles (25°, 27.5°, 30°, and 32.5°) were considered for the case with the highest turbulence intensity (i.e. Grid C with $TI = 3.44\%$). Unlike in [6], no thrust scaling was applied to the acoustic amplitudes. Hence, higher β values correspond to higher blade loading and higher thrust generation.

In total, this provides a total of seven stimuli (since the case of Grid C and $\beta = 30°$ is considered twice). The whole analysis was repeated for two different emission angles of $\theta = 90°$ and 140°, i.e., within the propeller plane and downstream, respectively. To assess the repeatability of the answers collected, six of the stimuli were presented twice to the participants. Therefore, each test subject listened to a total of 20 stimuli in a randomized order to mitigate, to some extent, potential learning effects. Since all sound recordings were quasi-stationary (i.e., with negligible variations over time), a total duration of 10 s per stimulus was deemed sufficient for the assessment.

4.3. Test subjects

A total of 32 test subjects participated in the listening experiment, comprising 15 men and 17 women. The average age of the participants was 34.2 years with a standard deviation of 11.1 years.

Regarding the level of education, three participants had a high school diploma as their highest level of education, whereas the rest held various degrees, such as BSc (2), MSc (21), and PhD (6). The subject group included one student, 29 people employed for wages, one self-employed person, and one retired person. Amongst the *'employed for wages'* group, four individuals worked at Delft University of Technology.

All participants reported feeling well, and their self-reported hearing level was high, with three indicating 'excellent', 13 indicating 'very good', and 15 indicating 'good', and only one indicating 'fair'. None of the participants had ear diseases or wore hearing aids, had a hearing accident in the

past, or had ever had tinnitus.

The responses provided by every pair of test subjects had strong cross-correlations, with average Pearson correlation coefficients of about $\rho = 0.717$, see Fig. 2(b). Moreover, the participant responses were found to be relatively self-consistent, with a root mean square difference of 1.06 points between the ratings collected for the repeated stimuli. In general, the absolute differences between the responses for all repeated sounds were below 2 points in 85% of the cases, which is deemed acceptable.

Overall, no relevant biases were found between the participants' responses and their demographics; thus, all 32 participants were considered in the psychoacoustic analysis henceforth.

5. RESULTS AND DISCUSSION

5.1. Influence of the inflow turbulence intensity

Figure 3(a) presents the comparison of the spectra for all grid (i.e. TI) cases, for $\beta = 30°$, and a polar emission angle of $\theta = 140°$, i.e. downstream of the propeller plane. The frequency axis is normalized with respect to the blade passing frequency (BPF = $Bf_r \approx 1$ kHz, where $B = 6$ is the blade count). Overall, increasing TI causes a noticeable rise in the broadband noise up to approximately the 7$^{\text{th}}$ BPF ($\approx$ 7 kHz). On the other hand, a considerable reduction in high-frequency broadband noise is observed for all the grid cases after the 11$^{\text{th}}$ BPF ($\approx$ 11 kHz). A similar reduction occurs for all grid cases.

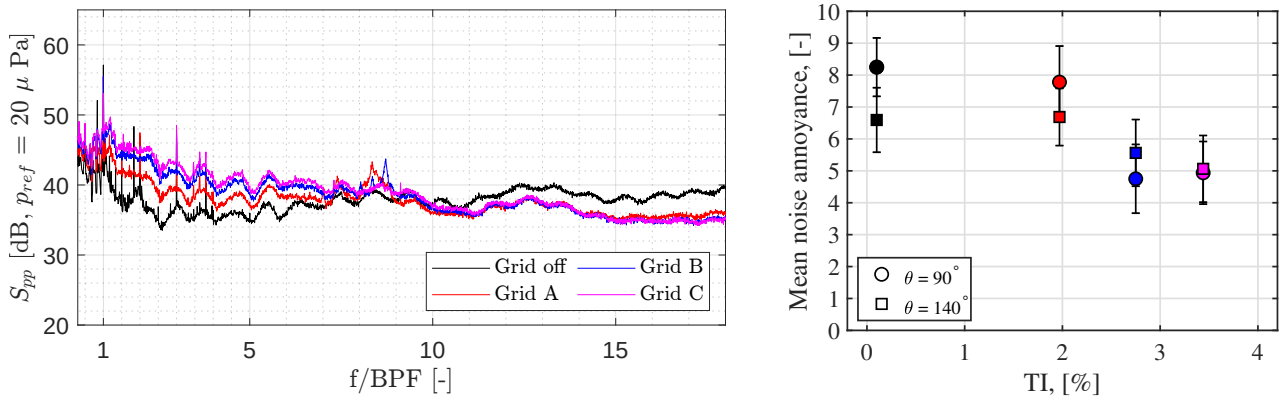

(a) (b)

Figure 3: (a) Power spectra S_{pp} of acoustic pressure for $\beta = 30°$ and all grid cases. All spectra correspond to $\theta = 140°$ ($\Delta f = 5$ Hz), without the −20 dB scaling. (b) Mean annoyance ratings for all grid cases and $\beta = 30°$. The error bars denote the standard deviations in the annoyance ratings.

The corresponding mean annoyance ratings for the cases with $\beta = 30°$ are depicted in Fig. 3(b) for the four grid cases. A distinction is made between the two emission angles of $\theta = 90°$ and 140°. It is observed that increasing the TI beyond 2% considerably reduces the perceived annoyance from mean ratings of 7 to 8 out of 10 to roughly 5 (i.e. approximately a 30% reduction). For the three lowest-turbulence cases, the sounds at $\theta = 90°$ (within the propeller rotation plane) were perceived as more annoying than those at $\theta = 140°$, although this difference decreased as TI rose. Interestingly, the psychoacoustic characterization of the same experimental test cases in [14] showed that most SQMs presented higher values at $\theta = 140°$ than at $\theta = 90°$, except for tonality K_5, which also presented decreasing values for increasing TI, unlike loudness-based metrics. Another SQM that also decreased to some extent with increasing TI was sharpness S_5 [14].

5.2. Influence of the collective blade pitch angle

In a similar way as in section 1, Fig. 4(a) presents the far-field noise emissions for all collective blade pitch angles β considered for the Grid C case and the same emission angle ($\theta = 140°$). In contrast to

the TI variation, increasing β mostly decreases the broadband noise emissions for frequencies higher than the 10$^{\text{th}}$ BPF ($\approx$ 10 kHz). On the other hand, the spectra below that threshold virtually remained constant for varying β angles.

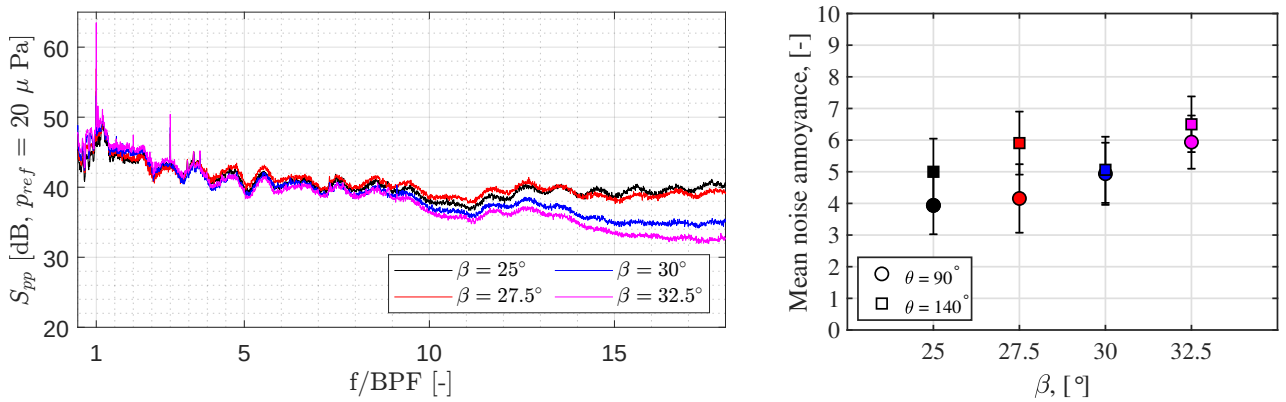

(a) (b)

Figure 4: (a) Power spectra S_{pp} of acoustic pressure for Grid C and all β cases. All spectra correspond to $\theta = 140°$ ($\Delta f = 5$ Hz), without the -20 dB scaling. (b) Mean annoyance ratings for all β cases and Grid C. The error bars denote the standard deviations in the annoyance ratings.

Figure 4(b) shows the mean annoyance ratings for varying β and Grid C. In general, it seems that increasing β also causes a gradual increase in the perceived annoyance, reaching its maximum values for $\beta = 32.5°$. This aligns with the aforementioned higher thrust generated at higher collective blade pitch angles and reflects the importance of loading noise mechanisms. Unlike the case with varying TI in Fig. 3(b), the stimuli corresponding to the emission angle of $\theta = 140°$ are evaluated as slightly more annoying than those within the propeller plane ($\theta = 90°$). This behaviour agrees with the directivity patterns of loudness N_5 discussed for the same experimental dataset in [14].

5.3. Annoyance modeling

A correlation analysis was conducted to assess the performance of several sound indicators (including conventional, sound quality, and psychoacoustic annoyance metrics) in explaining the variability of the annoyance ratings collected during the listening experiment. Table 2 contains the corresponding ranges of variation, Pearson correlation coefficients ρ (including the 95% confidence intervals), and p-values for each of the metrics considered. Figure 5 presents the correlation analyses of some of the sound metrics considered. In this figure, the marker fill colour corresponds to the grid case (i.e. TI) and the marker line colour denotes the collective blade pitch angle β. Circular markers correspond to $\theta = 90°$ and square markers to $\theta = 140°$. The least-squares fits are plotted as dashed blue lines, and the shaded blue areas correspond to the 95% confidence intervals.

Interestingly, when following the common criterion of having a p-value below 0.05 to consider a correlation statistically significant, all the energy-based and loudness-based metrics, such as the EPNL (see Fig. 5(a)) present p-values considerably higher than that threshold, indicating that they are not suitable predictors for noise annoyance for this particular application. Only tonality K_5 (see Fig. 5(b)) meets such a requirement, with $\rho = 0.779$ and a p-value of 0.001. This is rather unexpected, since several previous studies featuring wind turbines [28, 29], drones [9], UAM vehicles [30], and conventional aircraft [31] showed that the observed noise annoyance ratings were strongly dependent on metrics based on loudness and that the global psychoacoustic annoyance models usually outperformed individual metrics. On the other hand, Boucher *et al.* [32] conducted psychoacoustic listening experiments featuring auralized sounds from a quadrotor UAM vehicle and reported that (when loudness was kept constant) other sound quality metrics like tonality or roughness were positively correlated to the annoyance ratings. This phenomenon is likely to be due

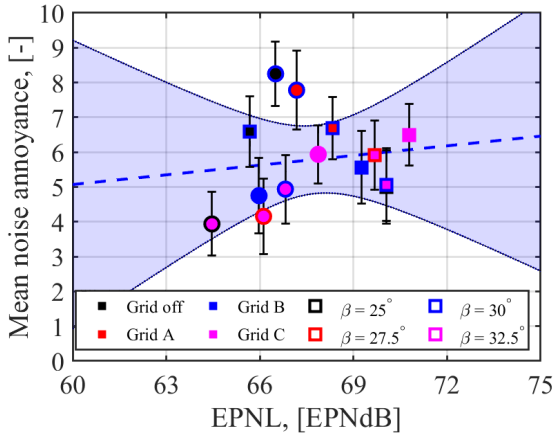

(a) EPNL (ρ = 0.142, p-value = 0.627)

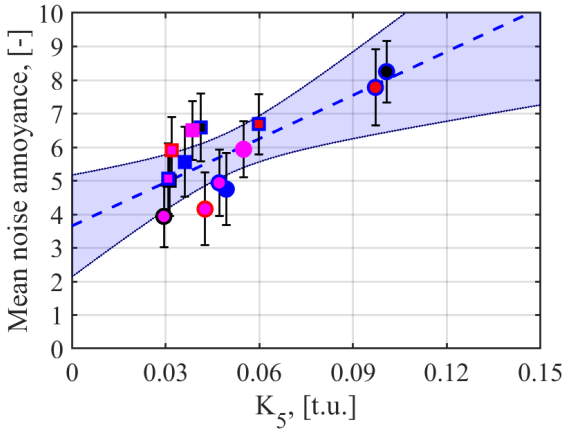

(b) K_5 (ρ = 0.779, p-value = 0.001)

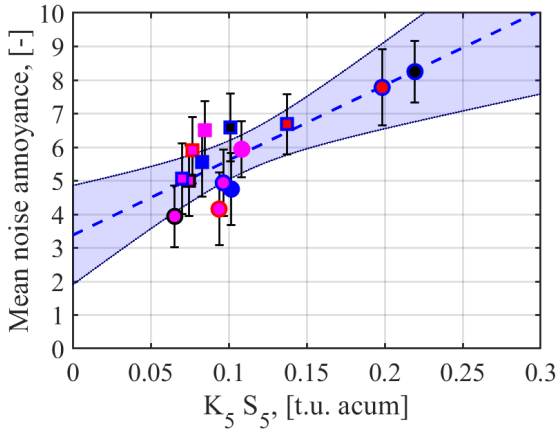

(c) $K_5\,S_5$ (ρ = 0.818, p-value = 3.5×10^{-4})

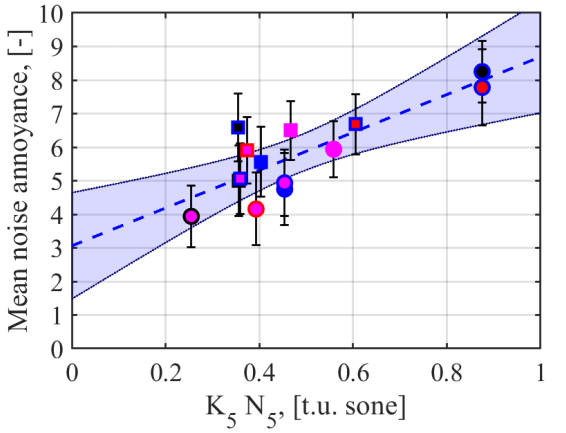

(d) $K_5\,N_5$ (ρ = 0.829, p-value = 2.5×10^{-4})

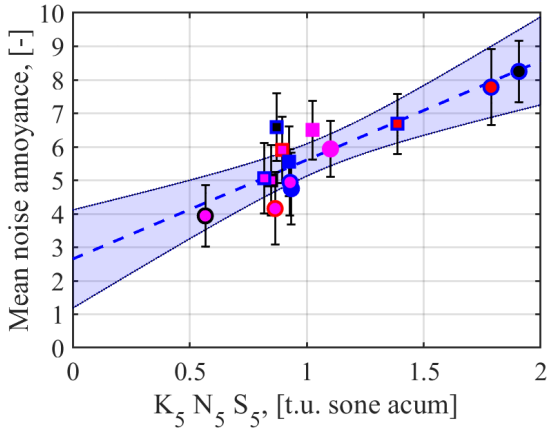

(e) $K_5\,N_5\,S_5$ (ρ = 0.875, p-value = 3.8×10^{-5})

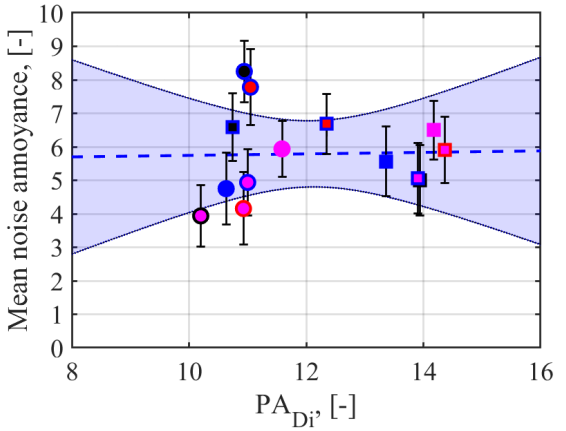

(f) $\mathrm{PA_{Di}}$ (ρ = 0.027, p-value = 0.927)

Figure 5: Correlation analysis between the mean annoyance ratings from the listening experiments and different sound metrics. The error bars denote the standard deviations in the annoyance ratings. The least-squares fits are plotted as dashed blue lines, and the shaded blue areas correspond to the 95% confidence intervals. Circular markers correspond to $\theta = 90°$ and square markers to $\theta = 140°$.

to the relatively complex nature of propeller noise with a combination of tonal noise, broadband components, partial masking between them, and, depending on the operating conditions, amplitude modulation over time. In the present study, however, all test cases featured the same rotational speed, so the variations of the R and FS metrics that evaluate the amplitude modulation were not as

Table 2: Pearson correlation coefficient ρ (including the 95% confidence interval) and associated p-values reported between the mean annoyance ratings and each of the sound metrics and psychoacoustic annoyance models.

Metric	**Range of variation**	ρ	**p-value**
$L_{p,eq}$, [dB]	65.96 – 71.48	−0.044 (−0.561 – 0.498)	0.881
$L_{p,A,eq}$, [dBA]	65.56 – 81.55	−0.037 (−0.557 – 0.503)	0.900
$PNLT_{max}$, [PNdB]	65.00 – 71.54	0.164 (−0.401 – 0.639)	0.575
EPNL, [EPNdB]	64.46 – 70.79	0.142 (−0.420 – 0.626)	0.627
N_5, [sone]	8.62 – 12.09	−0.101 (−0.600 – 0.454)	0.731
S_5, [acum]	1.97 – 2.46	−0.034 (−0.554 – 0.506)	0.910
K_5, [t.u.]	0.03 – 0.10	0.779 (0.424 – 0.927)	0.001
R_5, [asper]	0.05 – 0.08	−0.205 (−0.664 – 0.365)	0.482
FS_5, [vacil]	0.05 – 0.12	−0.334 (−0.734 – 0.239)	0.244
$K_5 S_5$, [t.u. acum]	0.07 – 0.22	0.818 (0.507 – 0.940)	3.5×10^{-4}
$K_5 N_5$, [t.u. sone]	0.25 – 0.88	0.829 (0.532 – 0.944)	2.5×10^{-4}
$K_5 N_5 S_5$, [t.u. sone acum]	**0.57 – 1.91**	**0.875 (0.647 – 0.961)**	$\mathbf{3.8 \times 10^{-5}}$
$PA_{Zwicker}$, [-]	9.98 – 14.28	−0.108 (−0.604 – 0.448)	0.713
PA_{More}, [-]	10.01 – 19.11	0.091 (−0.462 – 0.593)	0.756
PA_{Di}, [-]	10.2 – 14.37	0.027 (−0.511 – 0.550)	0.927

significant as for the other metrics.

Given the partial similarities in trends between the mean annoyance rating and loudness and sharpness aforementioned in sections 1 and 2, it was decided to investigate the potential correlation of the combined metrics $K_5 S_5$, $K_5 N_5$, and $K_5 N_5 S_5$ with the listening experiment responses, see Figs. 5(c-e). When using these combined metrics, even stronger correlations are observed, with ρ values of 0.818, 0.829, and 0.875, respectively, see Table 2. These results prove that, despite not being representative indicators of the reported noise annoyance in this particular application on their own, including the effects of sharpness and loudness, provides a more accurate model. Surprisingly, the PA model by Di *et al.*, which also includes the SQMs of tonality, sharpness, and loudness (although with a different nonlinear expression, as well as other metrics like R and FS) does not present a statistically significant correlation, see Fig. 5(f). In fact, most of the PA models available [22–24] are based on the following equation, where loudness is of the highest importance and the rest of SQMs play a secondary role:

$$\mathrm{PA} = N_5 \left(1 + \sqrt{\omega_S^2 + \omega_{FR}^2 + \omega_K^2}\right), \tag{1}$$

where ω_S, ω_{FR}, and ω_K, are, respectively, the terms related to sharpness, the combination of roughness and fluctuation strength, and tonality, which also include loudness in their formulas[3]. In addition, the whole parenthesis term is multiplied by N_5.

The current findings of this preliminary study, although limited to a relatively low number of cases, seem to indicate that the human perception of propeller noise is also highly dependent on its tonality and not so strongly on its loudness (i.e., the louder cases are not always the most annoying). Therefore, it is recommended to further investigate this phenomenon and to increase the importance of the tonality term in PA models dealing with propeller noise [32].

[3]The respective formulas to calculate these terms differ per PA model.

6. CONCLUSIONS

The present study documents the results of a listening experiment campaign featuring the noise emissions of an isolated propeller measured in aeroacoustic wind tunnel experiments. Different inflow turbulence intensity levels and collective blade pitch angles were evaluated.

It was reported that, while increasing the inflow turbulence intensity notably increases the broadband noise emissions (and, hence, the values of loudness-based metrics), this phenomenon in turn decreases the perceived tonality and sharpness. The combined effect results in lower perceived noise annoyance, partly explained by the highly tonal nature of propeller noise and its masking by the increase in broadband noise. Increasing the blade pitch angle, on the other hand, caused an increase in the mean annoyance ratings collected, despite the observed decrease in sharpness by the reduction in high-frequency noise content.

A correlation analysis between the mean annoyance ratings and different sound metrics showed the unexpected conclusion that only tonality was a statistically significant predictor of noise annoyance on its own. Combinations of this metric with other SQMs, like sharpness or loudness, further increased the predictive performance. This highlights the importance of tonality in the propeller noise emissions and that existing psychoacoustic annoyance models may need to increase the influence of the tonality term for assessing propeller noise. Moreover, increases in inflow turbulence were previously considered negative due to the observed increase in loudness-based metrics, but the present results seem to indicate that they might improve the perceived annoyance. Overall, this study is a valuable step for the perception-influenced design of devices equipped with propellers, such as drones or urban air mobility vehicles, to account for installation effects.

It should be considered, however, that the present study evaluated a relatively simple experimental setup with isotropic turbulence and a limited number of test conditions. Unfortunately, the limited number of observations performed limits the complexity of the noise annoyance prediction model achievable, to prevent overfitting. Future work should evaluate a more extensive parametric study featuring more sound stimuli and consider more realistic configurations, such as actual boundary layer ingestion systems or non-symmetric inflow conditions. In that way, more robust annoyance prediction models for propeller noise can be developed.

ACKNOWLEDGEMENTS

The authors would like to thank the 32 participants of the listening experiments for their time and effort.

This work is part of the HOPE (Hydrogen Optimized multi-fuel Propulsion system for clean and silEnt aircraft) project, and has received funding from the European Union's Horizon Europe research and innovation programme under grant agreement No. 101096275. Additionally, this publication is also a part of the *Listen to the future* project (project number 20247), a part of the Veni 2022 research programme (Domain Applied and Engineering Sciences). The latter project is granted to Roberto Merino-Martinez and is (partially) financed by the Dutch Research Council (NWO).

REFERENCES

1. R. M. Yupa-Villanueva, R. Merino-Martinez, A. Altena, and M. Snellen. Psychoacoustic Characterization of Multirotor Drones in Realistic Flyover Maneuvers. In 30^{th} *AIAA/CEAS Aeroacoustics Conference, June 4 – 7 2024, Rome, Italy*, 2024. AIAA paper 2024–3015.
2. S. A. Rizzi, D. L. Huff, D. D. Jr. Boyd, P. Bent, Henderson B., K. A. Pascioni, D. C. Sargent, D. L. Josephson, M. Marsan, B. He, and R. Snider. Urban Air Mobility Noise: Current Practice, Gaps, and Recommendations. Technical Report NASA Technical Memorandum 83199, NASA, 2020.
3. S. Schade, R. Merino-Martinez, P. Ratei, R. Bartels, S. and Jaron, and A. Moreau. Initial study on the impact of speed fluctuations on the psychoacoustic characteristics of a distributed propulsion

system with ducted fans. In *30 AIAA/CEAS aeroacoustics conference, june 4 – 7 2024, rome, italy*, 2024. tex.owner: rmerinomartine tex.timestamp: 2016.02.10.

4. F.d.N. Monteiro, R. Merino-Martinez, and L. T. Lima Pereira. Psychoacoustic Evaluation of an Array of Distributed Propellers Under Synchrophasing Operation. In 30th *AIAA/CEAS Aeroacoustics Conference, June 4 – 7 2024, Rome, Italy*, 2024. AIAA paper 2024–3321.
5. Feroz Ahmed, Carlos A. Ramos-Romero, Antonio J. Torija Martinez, and Mahdi Azarpeyvand. Boundary Layer Ingestion Ducted Fan: Aeroacoustic and Psychoacoustic Insights. In *30th AIAA/CEAS Aeroacoustics Conference (2024)*, Rome, Italy, June 2024. American Institute of Aeronautics and Astronautics.
6. L. N. Quaroni, R. Merino-Martinez, F. d. N. Monteiro, and S. S. Kumar. Collective blade pitch angle effect on grid turbulence ingestion noise by an isolated propeller. In 30th *AIAA/CEAS Aeroacoustics Conference, June 4 – 7 2024, Rome, Italy*, 2024. AIAA paper 2024–3209.
7. Edoardo Grande, Gianluca Romani, Daniele Ragni, Francesco Avallone, and Damiano Casalino. Aeroacoustic Investigation of a Propeller Operating at Low Reynolds Numbers. *AIAA Journal*, 60(2):860–871, February 2022.
8. A. J. Torija, C. Ramos-Romero, and N. Green. Acoustic and Psychoacoustic Characterisation of Unmanned Aircraft Systems as a Function of Vehicle Mass and Flight Procedure. In 30th *AIAA/CEAS Aeroacoustics Conference, June 4 – 7 2024, Rome, Italy*, 2024. AIAA paper 2024–3235.
9. R. Merino-Martinez, R. M. Yupa-Villanueva, B. von den Hoff, and J. S. Pockelé. Human response to the flyover noise of different drones recorded in field measurements. In 3rd *Quiet Drones conference, September 8 – 11 2024, Manchester, United Kingdom*, 2024.
10. R. Merino-Martinez, H. Ben-Gida, and M. Snellen. Psychoacoustic Evaluation of an Optimized Low–Noise Drone Propeller Design. In 30th *International Congress on Sound and Vibration (ICSV), July 8 – 11 2024, Amsterdam, the Netherlands*, 2024.
11. K. Heutschi, B. Ott, T. Nussbaumer, and P. Wellig. Synthesis of real world drone signals based on lab recordings. *Acta Acoustica*, 4(24):1–10, October 2020.
12. T. Sinnige, B. Della Corte, R. de Vries, F. Avallone, R. Merino-Martinez, D. Ragni, G. Eitelberg, and L. L. M. Veldhuis. Alleviation of Propeller–Slipstream–Induced Unsteady Pylon Loading by a Flow–Permeable Leading Edge. *Journal of Aircraft*, 56(3):1214–1230, May–June 2019. DOI: 10.2514/1.C035250.
13. Federico Petricelli, Paruchuri Chaitanya, Sergi Palleja-Cabre, Stefano Meloni, Phillip F. Joseph, Amin Karimian, Suresh Palani, and Roberto Camussi. An experimental investigation on the effect of in-flow distortions of propeller noise. *Applied Acoustics*, 214:109682, November 2023.
14. R. Merino-Martinez and L.N. Quaroni. Psychoacoustic characterization of an isolated propeller at different inflow turbulence conditions and collective pitch angles. In 11th *Forum Acusticum Euronoise Conference, June 23 – 26 2025, Málaga, Spain*, 2025.
15. R. Merino-Martinez, A. Rubio Carpio, L. T. Lima Pereira, S. van Herk, F. Avallone, M. Kotsonis, and D. Ragni. Aeroacoustic design and characterization of the 3D–printed, open–jet, anechoic wind tunnel of Delft University of Technology. *Applied Acoustics*, 170(107504):1–16, June 2020.
16. Nando Van Arnhem, Reynard De Vries, Tomas Sinnige, Roelof Vos, Georg Eitelberg, and Leo L. M. Veldhuis. Engineering Method to Estimate the Blade Loading of Propellers in Nonuniform Flow. *AIAA Journal*, 58(12):5332–5346, December 2020.
17. R. Amiet. Correction of open jet wind tunnel measurements for shear layer refraction. In *2nd Aeroacoustics Conference*, Hampton,VA,U.S.A., March 1975. American Institute of Aeronautics and Astronautics.

18. L.N. Quaroni and R. Merino-Martinez. Mitigation strategies for acoustic reflections generated by an axisymmetric wind tunnel nozzle. In 11th *Forum Acusticum Euronoise Conference, June 23 – 26 2025, Málaga, Spain*, 2025.
19. Lin Li, Haonan Zhu, Reza Maryami, Xianzhi Zhang, and Yu Liu. Flow and acoustic characterization of turbulence grids at wind tunnel nozzle exit. *Journal of Sound and Vibration*, 590:118535, November 2024.
20. R. Merino-Martinez. *Microphone arrays for imaging of aerospace noise sources*. PhD thesis, Delft University of Technology, 2018. ISBN: 978–94–028–1301–2.
21. G. F. Greco, R. Merino-Martinez, A. Osses, and S. C. Langer. SQAT: a MATLAB-based toolbox for quantitative sound quality analysis. In 52th *International Congress and Exposition on Noise Control Engineering, August 20 – 23 2023, Chiba, Greater Tokyo, Japan*. International Institute of Noise Control Engineering (I-INCE), 2023.
22. H. Fastl and E. Zwicker. *Psychoacoustics – Facts and models*. Springer Series in Information Sciences, Third edition, 2007. ISBN: 987–3–540–68888–4.
23. S. R. More. *Aircraft Noise Characteristics and Metrics*. PhD thesis, Purdue University, 2010. Report No. PARTNER–COE–2011–004.
24. Guo-Qing Di, Xing-Wang Chen, Kai Song, Bing Zhou, and Chun-Ming Pei. Improvement of Zwicker's psychoacoustic annoyance model aiming at tonal noises. *Applied Acoustics*, 105:164–170, 2016.
25. Gil Felix Greco, Roberto Merino-Martínez, and Alejandro Osses. SQAT: a sound quality analysis toolbox for MATLAB, January 2025. v1.2. Zenodo. DOI: 10.5281/ZENODO.14641811.
26. R. Merino-Martinez, B. von den Hoff, and D. G. Simons. Design and acoustic characterization of a psychoacoustic listening facility. In 29th *International Congress on Sound and Vibration (ICSV), July 9 – 13 2023, Prague, Czech Republic*, 2023.
27. J. S. Pockelé. Graphical User Interface for the Psychoacoustic Listening Laboratory (PALILA GUI), March 2025. v1.2.0. Zenodo. DOI: 10.5281/ZENODO.15100497.
28. R. Merino-Martinez, R. Pieren, and B. Schäffer. Holistic approach to wind turbine noise: From blade trailing–edge modifications to annoyance estimation. *Renewable and Sustainable Energy Reviews*, 148(111285):1–14, May 2021.
29. R. Merino-Martinez, R. Pieren, B. Schäffer, and D. G. Simons. Psychoacoustic model for predicting wind turbine noise annoyance. In 24th *International Congress on Acoustics (ICA), October 24 – 28 2022, Gyeongju, South Korea*, 2022.
30. R. Merino-Martinez and S. Schade. Psychoacoustic analysis of the perceptual influence of rotational speed fluctuations in an urban mobility vehicle with distributed ducted fans. In 54th *International Congress & Exposition on Noise Control Engineering (Inter-Noise), August 24 – 27 2025, Sao Paulo, Brazil*, 2025.
31. R. Merino-Martinez and V.S. Buzetelu. Aircraft noise-induced annoyance analysis using psychoacoustic listening experiments. In 11th *Forum Acusticum Euronoise Conference, June 23 – 26 2025, Málaga, Spain*, 2025.
32. M. A. Boucher, A. W. Christian, S. Krishnamurthy, T. Tracy, D. R. Begault, K. Shepherd, and S. A. Rizzi. Toward a Psychoacoustic Annoyance Model for Urban Air Mobility Vehicle Noise. Technical Report NASA TM–20240003202, NASA, June 2024.